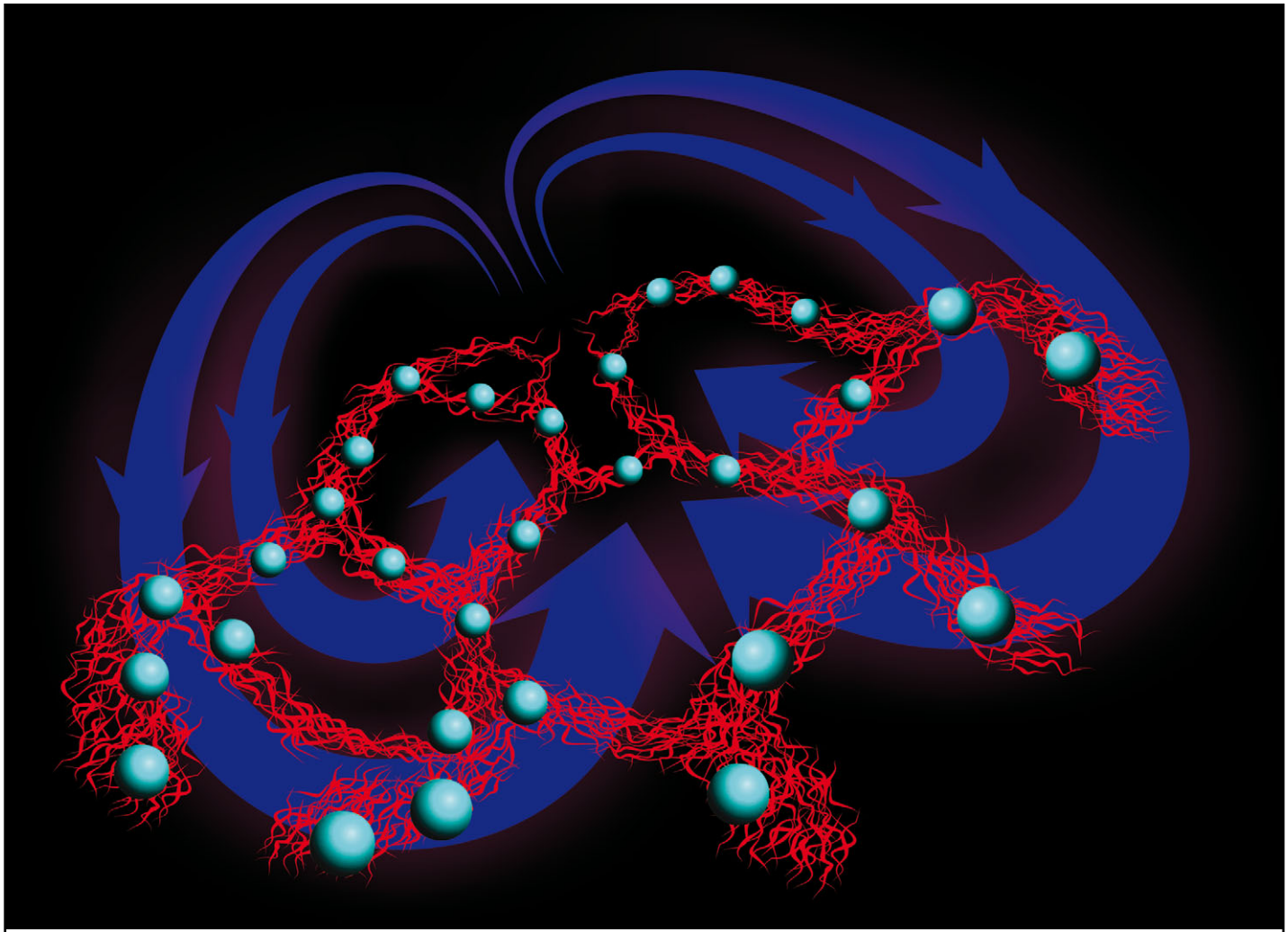

Showcasing work from the laboratory of Prof. Denise F. S. Petri, at the Institute of Chemistry, University of São Paulo, São Paulo, Brazil, and collaborative research groups from the University of São Paulo

Hybrid composites of xanthan and magnetic nanoparticles for cellular uptake

Novel composites of magnetite nanoparticles and xanthan networks present coercivity and are successful scaffolds for cell proliferation, particularly under the effect of an external magnetic field.

Artwork credit: Marcos Blasques @marcpbb

As featured in:

See Denise Freitas Siqueira Petri *et al.*, *Chem. Commun.*, 2013, **49**, 9911.

RSC Publishing

www.rsc.org/chemcomm

Registered Charity Number 207890

ChemComm

RSC Publishing

COMMUNICATION

View Article Online
View Journal | View Issue

Cite this: *Chem. Commun.*, 2013, **49**, 9911

Received 28th March 2013,
Accepted 4th June 2013

DOI: 10.1039/c3cc42277a

www.rsc.org/chemcomm

Hybrid composites of xanthan and magnetic nanoparticles for cellular uptake†

Vânia Blasques Bueno,[a] Anielle Martins Silva,[a] Leandro Ramos Souza Barbosa,[b] Luiz Henrique Catalani,[a] Érico Teixeira-Neto,[a] Daniel Reinaldo Cornejo[b] and Denise Freitas Siqueira Petri*[a]

We describe a fast and simple method to prepare composite films of magnetite nanoparticles and xanthan networks. The particles are distributed close to hybrid film surface, generating a coercivity of 27 ± 2 Oe at 300 K. The proliferation of fibroblast cells on the hybrid composites was successful, particularly when an external magnetic field was applied.

The success of magnetic particles in biomedical,[1,2] catalytic,[3] magnetic resonance imaging[4] and environmental[5] applications has gained the attention of many researchers. However, such applications are achieved when the magnetic particles are small enough (<100 nm) and protected by stabilizers, which avoid their aggregation or further oxidation.[6] Magnetite (Fe_3O_4) can be synthesized by co-precipitation, an easy and cheap method.[6] The resulting particles present a broad size distribution and poor colloidal stability. In order to overcome this drawback stabilizers are added to the synthesis; they adsorb chemically or physically on the particles, creating an electrostatic or a steric barrier. Polymers and surfactants are typical stabilizers.[3,6–8] Alternatively, magnetite particles can be distributed in a polymer matrix, creating nanocomposites. Magnetite/epoxy resin composites prepared by dissolution and curing presented dynamic magnetic properties similar to those of free magnetite; but the molecular dynamics of the polymeric matrix was affected by the presence of magnetic nanoparticles (filler content <10 vol%).[9] Nanocomposites of polyurethane (PU) and functionalized Fe_3O_4 or $CoFe_2O_4$ particles (filler content < 6 mass%) were prepared by casting formed elongated agglomerates uniformly distributed in the polymer matrix, retaining the superparamagnetic properties of Fe_3O_4.[10] Bringing together magnetic particles and polysaccharides tends to be a relevant strategy to develop magneto-responsive non-toxic renewable materials. For instance, magnetic electrospun chitosan nanofiber composites were developed for hyperthermia treatment of tumor cells.[11] Consecutive layers of chitosan, cellulose and chitosan were deposited onto magnetite particles to be applied as a reusable adsorbent system for heavy metal ions.[5] Xanthan solutions (6 g L^{-1}) have been used to increase the colloidal stability of magnetite particle dispersions, especially due to the increase in viscosity.[12] The release of albumin from a starch based hydrogel containing magnetite particles could be modulated by the application of an external field.[13] Carboxymethylated-cellulose, -pullulan and -dextran used as a coating for magnetite particles resulted in distinct responses upon interacting with tumor cells.[14]

In this work we present a ten minute synthesis (see ESI† for details) to obtain magnetite particles by co-precipitation under sonication (MP-US) at (24 ± 1) °C in the absence of any stabilizer and their characterization. For comparison magnetite particles were synthesized by co-precipitation at (75 ± 1) °C (MP-Heat) during one hour, following a conventional method.[6] Further cross-linked xanthan films[15] (see ESI† for details) were immersed in the MP-US dispersion for ten seconds at (24 ± 1) °C. The xanthan cross-linked films are interesting materials for biomedical and environmental applications due to their biocompatibility and non-toxicity.[15,16]

The main properties and characteristics of MP-US and MP-Heat are presented in ESI-1.† The X-ray diffractograms obtained for MP-US and MP-Heat correspond to the magnetite structure, in accordance with the JCPDS card number 19-0629. The mean particle size estimated for MP-US and MP-Heat from the Scherrer equation applied to the (311) diffraction plane amounted to 14 nm and 13 nm, respectively. The isoelectric points (pI) of dialyzed MP-US and MP-Heat particles were determined to be 6.5 ± 0.1 and 5.4 ± 0.1, respectively (ESI-1†) using potentiometric titration. The adsorption of ammonium ions on the MP-US particles might lead to the relative increase in pI, while in the case of MP-Heat the heat favors the evaporation of ammonia. FTIR spectra obtained for MP-US and MP-Heat support this hypothesis (ESI-1†) and show their typical bands.[17,18] The colloidal stability of MP-US and MP-Heat was evaluated at pH 5, 7 and 9 (ESI-1†). Regardless of the pH, the time required for MP-Heat dispersions to achieve 75% of integral transmitted light was 4.0 ± 0.4 min. On the other hand, MP-US dispersions presented higher colloidal stability than MP-Heat at

[a] *Instituto de Química, Universidade de São Paulo, Av. Prof. Lineu Prestes 748, 05508-000, São Paulo, Brazil. E-mail: dfsp@usp.br; Fax: +55 11 3815 5579; Tel: +55 11 3091 3831*

[b] *Instituto de Física, Universidade de São Paulo, São Paulo, Brazil*

† Electronic supplementary information (ESI) available. See DOI: 10.1039/c3cc42277a

pH 7 and 9; they took 24.0 ± 0.5 min and 35.0 ± 0.5 min, respectively, to achieve 75% of integral transmitted light. These findings indicate that above the pI MP-US are negatively charged and electrostatic repulsion enhances the colloidal stability. The same was not observed for MP-Heat, although electrostatic repulsion would be expected at pH 7 and 9. The MP-US particles are more stable because they are in average smaller than MP-Heat, as evaluated using dynamic light scattering (ESI†). The acoustic cavitation and shockwaves inherent to the US technique favor the formation of many nuclei and retard the particle growth.[19] MP-US adsorbed from aqueous dispersion at pH 7 onto xanthan covered Si wafers. The MP-US layer thickness and index of refraction were determined to be (30 ± 3) nm and 1.85 ± 0.09 using ellipsometry. The AFM image obtained for this layer shows tiny particles densely packed on the surface and some large aggregates made of small particles. The cross section analysis indicates particle size on the order of 15 nm (Fig. 1, right). The adsorbed MP-Heat particles formed a very heterogeneous layer, making them inadequate for ellipsometric and AFM analyses. The magnetization *versus* magnetic field curves obtained at 300 K for MP-Heat (ESI-1†) and MP-US (Fig. 1, left) indicated no coercivity. At this temperature, the experimental curves are well adjusted by a simple model in which each system is assumed to be formed by a superposition of superparamagnetic grains.[20] At 5 K MP-US (Fig. 1) and MP-Heat (ESI-1†) presented hysteresis and coercivity of 250 Oe and 225 Oe, respectively. The saturation magnetization obtained at 70 kOe was 76 and 71 emu g^{-1}, at room temperature, for MP-Heat and MP-US, which are typical values for magnetite nanostructures.

Crosslinking xanthan chains in the presence of citric acid leads to biocompatible networks with high crosslinking density, high acid resistance and alkaline sensibility.[15] Dried films of cross-linked xanthan chains (~80 μm thick) were immersed into the MP-US dispersions at pH 7 and (24 ± 1) °C for 10 seconds. The resulting MP-US xanthan film nanocomposites were rinsed three times with distilled water and freeze-dried for ICP analysis or dried in an oven at (50 ± 1) °C overnight for SQUID analyses. The MP-US xanthan films exhibited a coercivity of 27 ± 2 Oe at 300 K (Fig. 2a). This is an important finding because it shows that MP-US particles in the xanthan matrix have a spatial arrangement, which differs from that in the powder state, giving rise to coercivity at 300 K. The increase in the coercivity in systems of "diluted" nanoparticles was verified by theoretical[21] and experimental[22,23] studies. At 5 K the coercivity of MP-US in the xanthan matrix increased to 335 Oe. The blocking temperature was determined to be 280 K (ESI-2†). One should note that the σ value decreased to ~0.02 emu g^{-1} due to the dilution effect, since the content of iron in the freeze-dried composite was determined to be 0.4 ± 0.1 wt% using

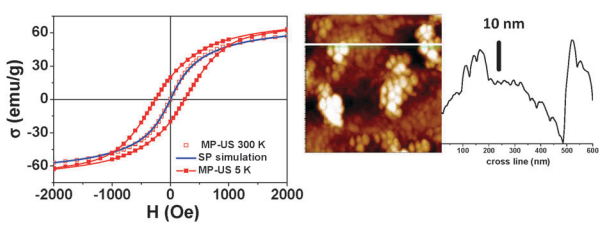

Fig. 1 Hysteresis loop determined for MP-US at 5 K and 300 K (blue solid line corresponds to simulations of superparamagnetic behavior) and AFM image with the corresponding cross-section obtained for the MP-US layer.

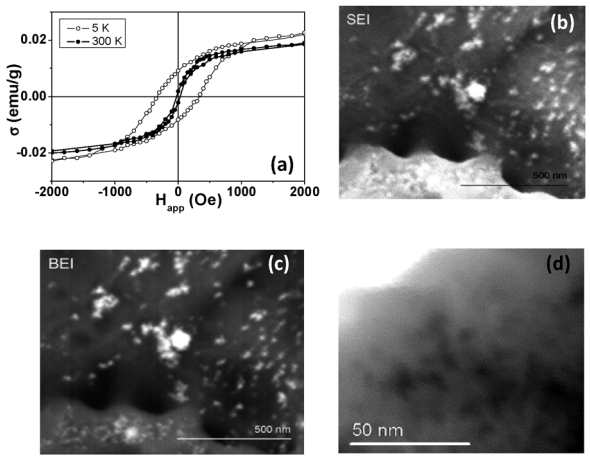

Fig. 2 MP-US xanthan composite films. (a) Hysteresis loop. (b) SEI and (c) BEI images of the same area of the nanocomposite surface. The atomic number sensitive BEI mode allows the distinction between the magnetite nanoparticles (bright spots) and the low atomic number xanthan film (dark gray background). (d) STEM image of thin edges of the nanocomposite surface. The nanometric black spots are individual magnetite nanoparticles adsorbed on the surface of the xanthan film.

ICP-AES analyses. At pH 7 the interactions between the xanthan matrix and magnetite are probably due to H bonding between xanthan hydroxyl groups and the hydroxyl groups on the magnetite surface. Systematic morphological investigation of the material using SEM showed the MP-US nanoparticles adsorbed throughout the nanocomposites surface, as shown in SEI (Fig. 2b) and BEI (Fig. 2c) images of a typical region of the nanocomposite surface. The individual MP-US nanoparticles shown in Fig. 2 appear as isolated or aggregated small bright spots, distributed throughout the film surface. High-resolution observation of many regions of the nanocomposite surface also showed (Fig. S3, ESI†) the presence of very small particles (size of a few tens of nanometers) individually deposited, along with particles and aggregates similar to those seen in Fig. 2.

The nanocomposite surface was also investigated in transmission, using the STEM mode, at very thin surface edges formed by the nanocomposite film tearing (Fig. S4, ESI†). The very small black spots shown in Fig. 2d are individual magnetite nanoparticles observed using STEM; similar distribution, of isolated nanoparticles very close to each other or forming small aggregates, is observed in many areas throughout the film surface. These particles appear to form a large population of individual magnetite nanoparticles, which are very close to each other, adsorbed on the xanthan surface. The possibility of the impregnation of nanoparticles within the xanthan film was carefully analyzed in cross-sections of the nanocomposite film (Fig. S4, ESI†); particles were not observed inside the film.

Hybrid magnetic materials have been successfully used for cellular uptake and tissue engineering.[24,25] The adhesion, viability, and proliferation of murine fibroblasts (3T3 L1) on MP-US xanthan film nanocomposites in the absence and presence of an external static magnetic field of 0.4 T (ESMF) during incubation was evaluated by MTT assay (ESI-5†). Cells were seeded with the same density on all scaffolds and after 1 d of culture they attached consistently, and proliferation was evaluated up to 7, 14 and 21 days. After 1 d bare xanthan networks (control experiments) and MP-US xanthan nanocomposites presented no cytotoxicity and cellular adhesion was not influenced by ESMF (Fig. 3).

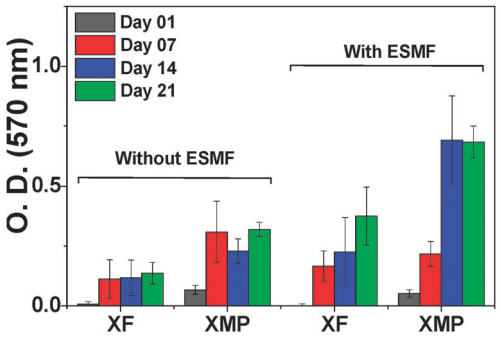

Fig. 3 MTT assay of fibroblasts on bare xanthan films (XF) and MP-US xanthan film nanocomposites (XMP) with and without exposure to external static magnetic field (ESMF).

Up to 7 days the cellular proliferation was similar for all systems, considering the standard deviations. After 14 days a higher increase in cellular proliferation was observed on the hybrid materials, which were exposed to ESMF. Under ESMF, increasing cellular growth on bare xanthan (control) was observed at 21 days, but it remained the same on MP-US xanthan films, probably due to growth saturation. In the absence of ESMF, the cellular growth extent was more pronounced on the hybrid films than on bare xanthan networks. The cellular growth behavior observed on MP-US xanthan composites without ESMF was comparable to that observed on bare xanthan with ESMF. Ca^{2+} ions, which are provided in the basal culture medium, are very important for intracellular signal transduction and metabolism. The amount of Ca^{2+} ions in the cells grown under the effect of ESMF was 5% larger than that determined for cells grown in the absence of ESMF (ESI†). ESMF can interact with the electric field of Ca^{2+} ions, favoring their permeation into the cell. Such interaction also influences other processes, for instance, the formation of mineral scales in drilling fluids or in hard water under ESMF,[26] and would explain the improved cell proliferation on bare xanthan films under ESMF. Although in the systems investigated here ESMF exerted no evident changes in the fibroblast morphological features (ESI-6†), literature reports indicate that ESMF might (i) increase the membrane permeability and the cell survival by inhibiting apoptosis,[27–29] (ii) induce osteogenesis[30–32] and morphogenesis,[33] (iii) increase the Ca^{2+} intracellular concentration[28] and (iv) alter the cellular format. Thus, it is possible that the events related to cell behavior under ESFM cited above and the cell proliferation on bare xanthan under ESFM are mainly due to the enhanced Ca^{2+} ions permeability. The presence of magnetic nanoparticles in the hybrid scaffold surface tends to increase the magnetic field, favoring this effect. Systematic experiments to evaluate the effect of increasing MP-US contents in the xanthan networks on the cellular proliferation and the corresponding intracellular Ca^{2+} concentration are under progress.

We have created a new, simple biocompatible nanocomposite from a renewable source, where magnetite nanoparticles assume a spatial distribution in the xanthan matrix, resulting in scaffolds with interesting magnetic properties and suitable for cell proliferation, particularly when exposed to ESMF.

Brazilian Funding agencies FAPESP (No. 2010/51219-4, No. 2010/13034-2), CNPq (No. 506510/2010-7, No. 471622/2010-9) and Rede Nanobiotec CAPES are gratefully acknowledged. We also thank LNNano-CNPEM (Campinas, Brazil) for the use of the FEI Inspect F50 SEM and Dr Edla M. A. Pereira for discussions.

Notes and references

1 A. K. Gupta and M. Gupta, *Biomaterials*, 2005, **26**, 3995.
2 Q. A. Pankhurst, J. Connolly, S. K. Jones and J. Dobson, *J. Phys. D: Appl. Phys.*, 2003, **36**, R167.
3 B. I. Kharisov, H. V. R. Dias, O. V. Kharissova, V. M. Jimenez-Perez, B. O. Pereza and B. M. Flores, *RSC Adv.*, 2012, **2**, 9325.
4 S. Mornet, S. Vasseur, F. Grasset, P. Verveka, G. Goglio, A. Demourgues, J. Portier, E. Pollert and E. Duguet, *Prog. Solid State Chem.*, 2006, **34**, 237.
5 Z. Liu, H. Wang, C. Liu, Y. Jang, G. Yu, X. Mu and X. Wang, *Chem. Commun.*, 2012, **48**, 7350.
6 A.-H. Lu, E. L. Salabas and F. Schüth, *Angew. Chem., Int. Ed.*, 2007, **46**, 1222.
7 A. L. Willis, N. J. Turro and S. O'Brien, *Chem. Mater.*, 2005, **17**, 5970.
8 B. L. Cushing, V. L. Kolesnichenko and C. J. O'Connor, *Chem. Rev.*, 2004, **104**, 3893.
9 B. Hallouet, B. Wetzel and R. Pelster, *J. Nanomater.*, 2007, **2007**, 1 article ID 34527.
10 N. Frickel, M. Gottlieb and A. M. Schmidt, *Polymer*, 2011, **52**, 1781.
11 T.-C. Lin, F.-H. Lin and J.-C. Lin, *Acta Biomater.*, 2012, **8**, 2704.
12 S. Comba and R. Sethi, *Water Res.*, 2009, **43**, 3717.
13 M. R. Guilherme, R. S. Oliveira, M. R. Mauricio, T. S. P. Cellet, G. M. Pereira, M. H. Kunita, E. C. Muniz and A. F. Rubira, *Soft Matter*, 2012, **8**, 6629.
14 J. Wotschadlo, T. Liebert, T. Heinze, K. Wagner, M. Schnabelrauch, S. Dutz, R. Müller, F. Steiniger, M. Schwalbe, T. C. Kroll, K. Höffken, N. Buske and J. H. Clement, *J. Magn. Magn. Mater.*, 2009, **321**, 1469.
15 V. B. Bueno, R. Bentini, L. H. Catalani and D. F. S. Petri, *Carbohydr. Polym.*, 2013, **92**, 1091.
16 S. Dimitriu, *Polysaccharides: Structural Diversity and Functional Versatility*, Marcel Dekker, New York, 2005.
17 N. Griffete, J.-F. Dechézelles and F. Scheffold, *Chem. Commun.*, 2012, **48**, 11364.
18 Y. Yamaguchi, M. Frisch, J. Gaw, H. F. Schaeffer and J. S. Brinkley, *J. Chem. Phys.*, 1986, **84**, 2262.
19 K. S. Suslick, Y. Didenko, M. M. Fang, T. Hyeon, K. J. Kolbeck, W. B. McNamara, M. M. Mdleleni and M. Wong, *Philos. Trans. R. Soc. London, Ser. A*, 1999, **357**, 335.
20 E. F. Ferrari, F. C. S. da Silva and M. Knobel, *Phys. Rev. B*, 1997, **56**, 6086.
21 D. Kechrakos and K. N. Trohidou, *J. Magn. Magn. Mater.*, 2003, **262**, 107.
22 S. Dutz and R. Hergt, *J. Nano- Electron. Phys.*, 2012, **4**, 2010.
23 A. F. Gross, M. R. Diehl, K. C. Beverly, E. K. Richman and S. H. Tolbert, *J. Phys. Chem. B*, 2003, **107**, 5475.
24 D. Depan and R. D. K. Misra, *Nanoscale*, 2012, **4**, 6325.
25 C. Cunha, S. Panseri, D. Iannazzo, A. Piperno, A. Pistone, M. Fazio, A. Russo, M. Marcacci and S. Galvagno, *Nanotechnology*, 2012, **23**, 465102.
26 A. Fathi, T. Mohamed, G. Claude, G. Maurin and B. A. Mohamed, *Water Res.*, 2006, **40**, 1941.
27 A. Chionna, M. Dwikat, E. Panzarini, B. Tenuzzo, E. C. Carlà, T. Verri, P. Pagliara, L. Abbro and L. Dini, *Eur. J. Histochem.*, 2003, **47**, 299.
28 C. Fanelli, S. Coppola, R. Barone, C. Colussi, G. Gualandi, P. Volpe and L. Ghibelli, *FASEB J.*, 1999, **13**, 95.
29 L. Potenza, L. Ubaldi, R. De Sanctis, R. De Bellis, L. Cucchiarini and M. Dachà, *Mutat. Res.*, 2004, **561**, 53.
30 N. Bock, A. Riminucci, C. Dionigi, A. Russo, A. Tampieri, E. Landi, V. A. Goranov, M. Marcacci and V. Dediu, *Acta Biomater.*, 2010, **6**, 786.
31 A. Tampieri, E. Landi, F. Valentini, M. Sandri, T. D'Alessandro, V. Dediu and M. Marcacci, *Nanotechnology*, 2011, **22**, 015104.
32 M. Levin, *Bioelectromagnetics*, 2003, **24**, 295.
33 J.-X. Yang, W. L. Tang and X.-X. Wang, *Cytotherapy*, 2010, **11**, 251.